DOI: 10.61782/fa.2023.1155

forum acusticum 2023

INITIAL CONDITIONS IMPACT ON NONLINEAR DYNAMICS OF A LOUDSPEAKER

Rahim Vesal[1] **Xinxin Guo**[1] **Hervé Lissek**[1*]
[1] Signal Processing Laboratory 2, EPFL, Switzerland

ABSTRACT

In contrast with linear systems, forced oscillations at particular frequencies may result in more than one stable limit cycle in the dynamic response of a nonlinear system. Also known as jump phenomenon, in these frequency regions, a nonlinear system would exhibit various dynamic behaviors critically depending on the initial conditions. The current study investigates the impact of initial conditions on nonlinear oscillations of an acoustically excited electro-acoustic viscoelastic membrane. Accordingly, a mathematical model is developed to simulate the nonlinear dynamics of the membrane, and the method of multiple scales is then utilized to solve the governing equation of motion of the system. Frequency response of the system is extracted to examine the effect of system nonlinearity level on jump phenomenon. Various combinations for initial states of the membrane are taken into consideration, and corresponding phase portraits are provided to study the dynamic response of the system in the jump region. Finally, basins of attraction for stable oscillations are mapped in a plane spanned by initial conditions of the system for different excitation frequencies.

Keywords: *jump phenomenon, nonlinear oscillations, nonlinear electroacoustic resonators, method of multiple scales, basins of attraction*

1. INTRODUCTION

Previous studies on active electroacoustic resonators (ERs) have mostly been carried out with the assumption that fluctuations in acoustic parameters remain small enough to maintain linearity, particularly at low frequencies. However, nonlinear resonators may also offer compelling performance characteristics that contribute to a diverse array of interesting phenomena. For example, the integration of a primary linear system with a nonlinear resonator offers opportunities to improve vibration mitigation through kinetic energy pumping [1-3] or addressing vibro-acoustic challenges by targeted energy transfer [4]. Despite the promising potential demonstrated by tunable nonlinear acoustic resonators, particularly in the context of enhanced active sound absorption [5], their comprehensive exploration and understanding have not been extensively pursued, revealing a notable research gap except for a limited number of recent investigations [6].

One of the most intriguing phenomena observed in nonlinear systems is the jump phenomenon. As a fundamental nonlinear behavior, it refers to the emergence of multiple stable states or branches in an oscillatory system frequency response, each representing a different dynamic regime [7-9]. The dynamic response of a nonlinear system is known to exhibit strong sensitivity to the initial conditions within the jump frequency region. While the impact of initial conditions in nonlinear dynamics of oscillators has been extensively studied, initial condition dependency of steady-state response of nonlinear ERs has not been addressed yet.

The current research endeavors to develop a numerical simulation to bridge the gap. Accordingly, the single-degree-of-freedom controllable dynamics of an ER is taken into consideration. The control methodology is implemented by supplying the resonator with a feedback control current, allowing for the realization of a tunable cubic nonlinearity for the system. The method of multiple scales is utilized to solve the governing nonlinear dynamic equation. Frequency response is presented to illustrate the effect of system nonlinearity on the jump phenomenon. Phase plane trajectories are depicted to demonstrate high sensitivity of the system dynamics to very small changes of the initial conditions. Finally, attraction basins are provided, which

[*] ***Corresponding author***: *herve.lissek@epfl.ch.*

represent particular sets of initial conditions that correspond with different steady-state responses in the jump region.

2. MATHEMATICAL MODELING

With a limited excitation level in the low frequency range, the dynamic behavior of an electroacoustic resonator (ER) could be conveniently modeled as a linear single-degree-of-freedom (SDOF) mass-spring-damper (MSD) system as [5]:

$$m_{\mathrm{ms}}\ddot{\xi}(t) = S_{\mathrm{m}}P_{\mathrm{f}}(t) - R_{\mathrm{ms}}\dot{\xi}(t) - \frac{\xi(t)}{C_{\mathrm{mc}}} - Bli(t), \quad (1)$$

where, a moving diaphragm with a mass of m_{ms} is backed with an enclosure of volume V_{b}, and supported by a viscoelastic suspension of mechanical compliance C_{ms} and resistance R_{ms}. Here, $\xi(t)$ represents the displacement of the moving diaphragm, and $C_{\mathrm{mc}} = C_{\mathrm{ms}}V_{\mathrm{b}}/(V_{\mathrm{b}} + \rho c^2 S_{\mathrm{m}}^2 C_{\mathrm{ms}})$ accounts for the fluid compressibility on the rear face of the diaphragm, while ρ, c and S_{m} denote air density, sound speed and the effective area of loudspeaker membrane, respectively. Also, $P_{\mathrm{f}}(t)$ indicates the total acoustic pressure applied to the front face of the membrane, Bl is the force factor of the moving coil transducer, and $i(t)$ shows the electric current circulating in it.

The linear relationship between the membrane displacement and acoustic pressure inside the back cavity of the loudspeaker, $P_{\mathrm{b}}(t)$, in the low frequency range provides the opportunity to define a control law for $i(t)$ as an arbitrary function of $\xi(t)$ through a feedback signal from $P_{\mathrm{b}}(t)$ simply using a microphone [5]. Here, the loudspeaker is subjected to an adjustable control current with a cubic nonlinearity in terms of membrane displacement as:

$$i(t) = \alpha G_{\mathrm{c}}[G_{\mathrm{m}}P_{\mathrm{b}}(t)]^3 = \beta_{\mathrm{nl}}\xi^3(t), \quad (2)$$

where $\beta_{\mathrm{nl}} = \alpha G_{\mathrm{c}}\left(G_{\mathrm{m}}C_{\mathrm{pd}}\right)^3$, C_{pd} is ratio of P_{b} to ξ, and α is a tunable nonlinear parameter, while G_{m} demonstrates the sensitivity of the microphone, and G_{c} is the voltage-to-current converter gain. This nonlinear control methodology allows for a desired level of nonlinearity in the system simply by tuning α, without the need for large excitation levels [5]. The latter expression for control current in Eqn. (2) can be substituted in Eqn. (1) to give the final equation of motion of the system as follows:

$$m_{\mathrm{ms}}\ddot{\xi}(t) + R_{\mathrm{ms}}\dot{\xi}(t) + \frac{\xi(t)}{C_{\mathrm{mc}}} + Bl\beta_{\mathrm{nl}}\xi^3(t) = S_{\mathrm{m}}P_{\mathrm{f}}(t). \quad (3)$$

Considering the loudspeaker being exposed to acoustic excitation at one end of an impedance tube, $P_{\mathrm{f}}(t)$ can be expressed as a summation of incident $P_{\mathrm{inc}}(t)$ and reflected $P_{\mathrm{ref}}(t)$ pressure waves. Here, it should be noted that the behavior of the system under a desired external excitation, e.g., a pure tonal excitation, would be impossible to analyze with the current format of Eqn. (3) due to the presence of higher harmonics in the reflected waves, especially when the system response exhibits unpredictable transitions in the jump frequency region.

Therefore, a preferable alternative would be to take the planar wave propagation assumption into account to represent $P_{\mathrm{f}}(t)$ as [10]:

$$P_{\mathrm{f}}(t) = P_{\mathrm{inc}}(t) + P_{\mathrm{ref}}(t) = 2P_{\mathrm{inc}}(t) - \frac{\rho c S_{\mathrm{m}}}{S_{\mathrm{d}}}\dot{\xi}(t), \quad (4)$$

where S_{d} denotes the cross-section area of the tube. Eqn. (4) can then be substituted in Eqn. (3) to give:

$$\ddot{\xi}(t) + \left(\frac{R_{\mathrm{ms}}}{m_{\mathrm{ms}}} + \frac{\rho c S_{\mathrm{m}}^2}{m_{\mathrm{ms}}S_{\mathrm{d}}}\right)\dot{\xi}(t) + \frac{\xi(t)}{m_{\mathrm{ms}}C_{\mathrm{mc}}} + \frac{Bl\beta_{\mathrm{nl}}}{m_{\mathrm{ms}}}\xi^3(t) = 2\frac{S_{\mathrm{m}}}{m_{\mathrm{ms}}}P_{\mathrm{inc}}(t). \quad (5)$$

2.1 Perturbation analysis

Here, the method of multiple scales is utilized in order to solve the nonlinear governing equation of the problem. However, it is beneficial to first present a nondimensional form of Eqn. (5) to provide a better understanding of the problem from a physical point of view. Accordingly, the dimensionless counterparts of time and the diaphragm displacement are introduced as $\tau = \hat{\omega}t$ and $x = \xi/\hat{\xi}$ respectively, where $\hat{\omega} = 1/\sqrt{m_{\mathrm{ms}}C_{\mathrm{mc}}}$ represents the natural frequency of the system, and $\hat{\xi}$ is a reference value for the displacement measurement. Considering an incident pressure of the form $P_{\mathrm{inc}}(t) = \hat{P}\cos(\omega t)$, the nondimensionalized form of Eqn. (5) can be obtained as follows:

$$\frac{d^2x}{d\tau^2} + \varepsilon C\frac{dx}{d\tau} + x + \varepsilon k_{\mathrm{nl}}x^3 = 2\varepsilon P_0\cos(\Omega\tau), \quad (6)$$

where, $\varepsilon \ll 1$ is an arbitrary chosen dimensionless small perturbation parameter that points out the relatively low-order magnitude of energy dissipation, nonlinearity, and excitation level in the system. Also, $\Omega = \omega/\hat{\omega}$ represents the dimensionless excitation frequency, while $C = (R_{\mathrm{ms}}S_{\mathrm{d}} + \rho c S_{\mathrm{m}}^2)/\varepsilon\hat{\omega}m_{\mathrm{ms}}S_{\mathrm{d}}$, $k_{\mathrm{nl}} = Bl\beta_{\mathrm{nl}}\hat{\xi}^2/\varepsilon\hat{\omega}^2 m_{\mathrm{ms}}$, and $P_0 = S_{\mathrm{m}}\hat{P}/\varepsilon\hat{\xi}\hat{\omega}^2 m_{\mathrm{ms}}$ are introduced as nondimensional counterparts of damping factor, nonlinear stiffness, and excitation amplitude, respectively.

Current study aims to investigate the response of the system in the vicinity of the natural frequency, which is equal to 1 for the linear part of the nondimensional differential equation

(6). Therefore, the excitation frequency is considered as follows:

$$\Omega = 1 + \varepsilon\sigma, \tag{7}$$

where, σ is the detuning parameter. Following the standard solution procedure with MMS, the following expansion is assumed for the response to determine an approximation for the solution [11]:

$$x(\tau, \varepsilon) = x_0(T_0, T_1) + \varepsilon x_1(T_0, T_1) + O(\varepsilon^2), \tag{8}$$

where, $T_0 = \tau$ is the fast time scale, $T_1 = \varepsilon\tau$ refers to the slow time scale, and derivatives with respect to τ can be defined as:

$$\frac{d}{d\tau} = D_0 + \varepsilon D_1 + O(\varepsilon^2), \tag{9}$$

$$\frac{d^2}{d\tau^2} = D_0^2 + 2\varepsilon D_0 D_1 + O(\varepsilon^2), \tag{10}$$

where $D_n = \partial/\partial T_n$. Substitution of Eqns. (7), (8), (9) and (10) in (6) returns the following two equation for different orders of ε.

ε^0:

$$\varepsilon^0: \quad D_0^2 x_0 + x_0 = 0, \tag{11}$$

$$\varepsilon^1: \quad D_0^2 x_1 + x_1 = -2D_0 D_1 x_0 - C D_0 x_0 - k_{\mathrm{nl}} x_0^3 + 2P_0 \cos(T_0 + \sigma T_1), \tag{12}$$

The solution to Eqn. (11) can be assumed as:

$$x_0(T_0, T_1) = A(T_1) e^{iT_0} + \bar{A}(T_1) e^{-iT_0}, \tag{13}$$

where $\bar{A}$ is the complex conjugate of A. Substituting (13) in (12) gives:

$$D_0^2 x_1 + x_1 = -2i\acute{A} e^{iT_0} - iCA e^{iT_0} - 3k_{\mathrm{nl}} A^2 \bar{A} e^{iT_0} + P_0 e^{i\sigma T_1} e^{iT_0} + \mathrm{cc} + \mathrm{NST}, \tag{14}$$

where $\acute{A}$ expresses the derivative of A with respect to T_1, and cc and NST account for the complex conjugate and non-secular terms. Satisfying the solvability condition demands secular terms to be eliminated, which means that the sum of the first four terms in the right-hand side of (14) with e^{iT_0} must be set equal to zero. Accordingly, with $A(T_1)$ represented in polar form as $A(T_1) = \frac{1}{2} a(T_1) e^{i\theta(T_1)}$, one can achieve at the following equation:

$$i\acute{a} - \sigma a + \acute{\eta} a + ia\frac{C}{2} + \frac{3}{8} k_{\mathrm{nl}} a^3 = P_0 e^{i\eta}, \tag{15}$$

where $\eta = \sigma T_1 - \theta$. The steady state solution can eventually be achieved through the summation of squared values of real and imaginary parts of Eqn. (15), after trimming off the terms with time derivatives, which gives a nonlinear algebraic equation for $a(T_1)$ as:

$$\frac{9}{64} k_{\mathrm{nl}}^2 a^6 - \frac{3}{4} \sigma k_{\mathrm{nl}} a^4 + \left(\frac{C^2}{4} + \sigma^2\right) a^2 = P_0^2, \tag{16}$$

Dimensionless positive displacement amplitude a can then be obtained from Eqn. (16) for different values of σ. Considering the polar form of $A(T_1)$, the acquired value for a would be equal to the amplitude of x_0 according to Eqn. (13), and consequently x in Eqn. (8) neglecting the terms with higher orders of ε. The actual displacement of the loudspeaker along with the stimulation frequency can then be achieved by $\xi = \hat{\xi} x$ and $\omega = \hat{\omega}\Omega$, respectively.

3. NUMERICAL SIMULATION AND RESULTS

The parameters of the ER can be determined through calibration measurements as explained in detail for example in [12]. A showcase study is presented here to investigate the nonlinear dynamics of a commercially available electrodynamic loudspeaker (Visaton FRWS 5 SC). It is noteworthy that characterization of an ER parameters can be determined through calibration measurements as explained in detail for example in [12]. The numerical values of the ER characteristics as well as all other affecting parameters are listed in Tab. 1.

Table 1. Input parameters.

Parameter	Numerical value	Parameter	Numerical value
m_{ms}	0.618 g	S_{d}	25 cm^2
R_{ms}	0.2806 Ns.m^{-1}	S_{m}	12 cm^2
Bl	1.1141 N.A^{-1}	C_{mc}	0.2174 mm.N^{-1}
ρ	1.2047 kg.m^{-3}	$\hat{P}$	0.2 Pa
c	343.2 m.s^{-1}	G_{c}	0.0095 A.V^{-1}
C_{pd}	1.21e6 N.m^{-3}	G_{m}	-0.36 V.Pa^{-1}

Moreover, the perturbation parameter ε is set equal to $0.01\, R_{\mathrm{ms}}/m_{\mathrm{ms}}\hat{\omega}$, while $\hat{\xi} = 0.1$ µm is assumed for nondimensionalizing. A Matlab code was developed to solve the nonlinear governing equation of problem. It is important to note that the solution to the nonlinear algebraic equation (16) may yield either one or three positive values for a, depending on the value of α. To visualize the system's frequency response near the natural frequency, Fig. 1 showcases the results obtained for different values of α.

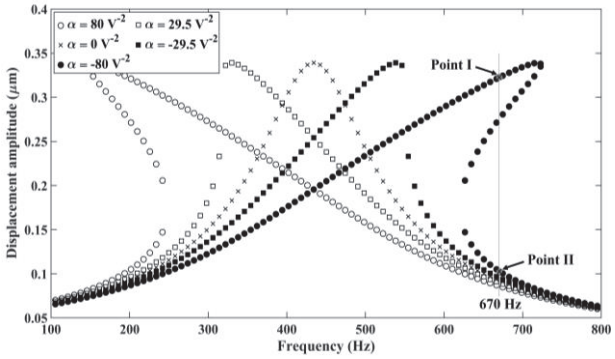

Figure 1. Comparison of the ER frequency response for different values of tunable nonlinear parameter α.

The ER may exhibit hardening or softening behavior depending on the sign of α. When the magnitude of α exceeds a specific threshold ($|\alpha| > 29.5\ \mathrm{V}^{-2}$), the nonlinear nature of the system manifests as a distinct bending of the response curve, resulting in the emergence of multivalued amplitudes within a specific frequency range. Commonly known as the jump phenomenon, this intriguing behavior signifies the high sensitivity of the response of a nonlinear system to variations in initial conditions [13]. Subsequent simulations are carried out considering a hardening cubic stiffness with a constant value of $\alpha = -80\ \mathrm{V}^{-2}$.

Considering the real and imaginary parts of Eqn. (15), it can be shown that there exists a unique corresponding pair of a and η that precisely represent any arbitrary chosen combination of system initial states (initial position and velocity).

Fig. 2 depicts the phase portrait trajectories of the diaphragm oscillation amplitude, $\bar{a} = \hat{\xi}a$, for two slightly different initial states of a and η under excitation frequency of 670 Hz, which correspond to points I and II on the frequency response curve in Fig. 1. It is evident that the system dynamic behavior is strongly dependent on the initial conditions and small changes in initial states can severely change the system dynamics. It is worthwhile to note that nodes in Fig. 2 correspond to stable limit cycles where the oscillation amplitude converges to a fixed value. To demonstrate the relationship between the steady-state oscillation amplitude and the initial conditions of the system, the basins of attraction for stable solutions of Eqn. (15) are depicted in Figs. 3, 4, and 5 for excitation frequencies of 630, 670, and 730, respectively.

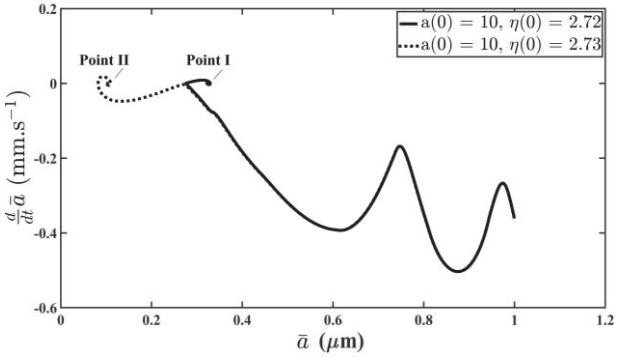

Figure 2. Oscillation amplitude phase portrait for different initial conditions.

These figures illustrate the mapping of results onto a plane spanned by initial conditions. Here, black sections indicate initial conditions that lead the steady-state response of the system toward the upper branch in the jump frequency region, while white parts are attributed with lower oscillation amplitudes.

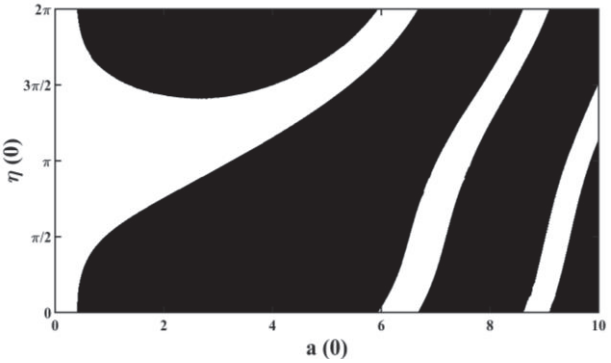

Figure 3. Basins of attraction at 630 Hz.

The first conclusion one can come up with from Figs. 3, 4, and 5, a notable observation is the periodicity of the results with respect to η, which is due to polar representation of $A(T_1)$. Furthermore, it is evident that the system exhibits high sensitivity to initial conditions, particularly in the vicinity of the basins' boundaries. Given the inherent limitations in precision associated with commercially available measurement tools, the steady-state dynamic behavior of the system can only be statistically estimated rather than precisely predicted in these regions under realistic conditions.

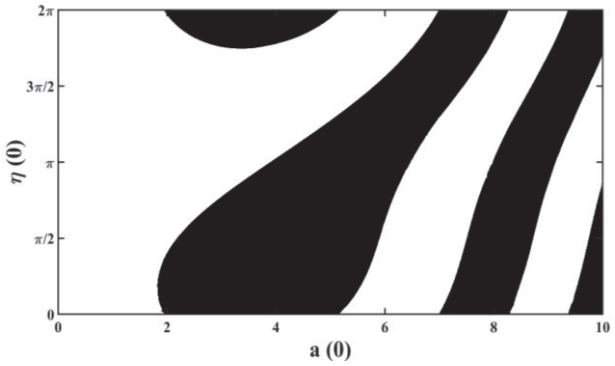

Figure 4. Basins of attraction at 670 Hz.

Finally, the comparison of Figs. 3, 4, and 5 highlights emerging a prominent trend. The expansion of the white basins indicates a higher probability of the steady-state response to converge towards the lower branch by increasing the excitation frequency in the jump region. It is evident that the system may exhibit the tendency to converge to either of the branches across the entire jump frequency region. Nevertheless, this observation highlights a discernible relationship between the excitation frequency and the likelihood of the loudspeaker diaphragm steady-state behavior in the jump region.

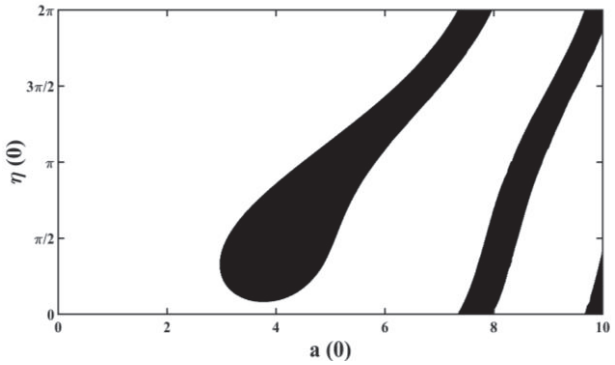

Figure 5. Basins of attraction at 720 Hz.

4. CONCLUSION

A mathematical model of nonlinear dynamics of a feedback current-controlled electroacoustic resonator is developed and numerically solved using the method of multiple scales. Jump Phenomenon is observed in the frequency response as soon as the system nonlinearity exceeds a specific threshold. The results reveal a strong connection between the initial conditions and the steady-state response of the system in the jump frequency region, where a slight change in initial conditions may drive the phase plane trajectories towards different stable limit cycles. Lastly, increased likelihood of the steady-state response is observed to converge to the lower branch of the frequency response by increasing the excitation frequency in the jump region. The current research highlights the significance of initial conditions in dynamics of acoustically excited nonlinear ERs dynamics, providing hopefully useful insights for further advancements in the field.

5. REFERENCES

[1] G. Sigalov, O.V. Gendelman, M.A. Al-Shudeifat, L.I. Manevitch, A.F Vakakis, and L.A. "Bergman, Resonance captures and targeted energy transfers in an inertially-coupled rotational nonlinear energy sink," *Nonlinear dynamics*, Vol. 69, pp1693-704, 2012.

[2] P.Y. Bryk, S. Bellizzi, R. Côte, "Experimental study of a hybrid electro-acoustic nonlinear membrane absorber," *Journal of Sound and Vibration*. Vol. 23, no. 424, pp. 224-37, 2018.

[3] R. Côte, M. Pachebat, and S. Bellizzi, "Experimental evidence of simultaneous multi-resonance noise reduction using an absorber with essential nonlinearity under two excitation frequencies" *Journal of sound and vibration*. Vol. 333, no. 20, pp. 5057-76, 2014.

[4] S.M. Hasheminejad, and R. Vesal, "Numerical simulation of impact sound transmission control across a smart hybrid double floor system equipped with a genetically-optimized NES absorber," *Applied Acoustics*. Vol. 182, pp 108179.

[5] X. Guo, H. Lissek, and R. Fleury, "Improving sound absorption through nonlinear active electroacoustic resonators," *Physical Review Applied*, vol. 13, no. 1, pp. 014018, 2020.

[6] D. Bitar, E. Gourdon, C.H. Lamarque, and M. Collet, "Shunt loudspeaker using nonlinear energy sink," *Journal of Sound and Vibration*. vol. 15, no. 456, pp. 254-71, 2019.

[7] M. Rezaee, and R. Vesal, "Perturbation analysis of resonant and non-resonant excitations of a beam equipped with a nonlinear vibration absorber," *Iranian Journal of Mechanical Engineering*, vol. 20, no. 3, pp. 109-32, 2018.

[8] Z.N. Ahmadabadi, and S.E. Khadem, "Nonlinear vibration control of a cantilever beam by a nonlinear

energy sink," *Mechanism and Machine Theory*, vol. 50, pp. 134-49, 2012.

[9] A.E. Mamaghani, S.E. Khadem, and S. Bab, "Vibration control of a pipe conveying fluid under external periodic excitation using a nonlinear energy sink," *Nonlinear Dynamics*, vol. 86, pp. 1761-95, 2016.

[10] L.E. Kinsler, A.R. Frey, A.B. Coppens, and J.V. Sanders: *Fundamentals of acoustics*. John Wiley & Sons, 2000.

[11] A.H. Nayfeh and B. Balachandran: *Applied nonlinear dynamics: analytical, computational, and experimental methods*. John Wiley & Sons, 2008.

[12] E. Rivet, "Room Modal Equalisation with Electroacoustic Absorbers," *Ecole Polytechnique Fédérale de Lausanne*, Ph.D. thesis, 2016.

[13] A.H. Nayfeh and D.T. Mook: *Nonlinear oscillations*. John Wiley & Sons, 2008.